Volume 18
Number 3
September 3, 2013

Cell Metabolism

www.cellpress.com

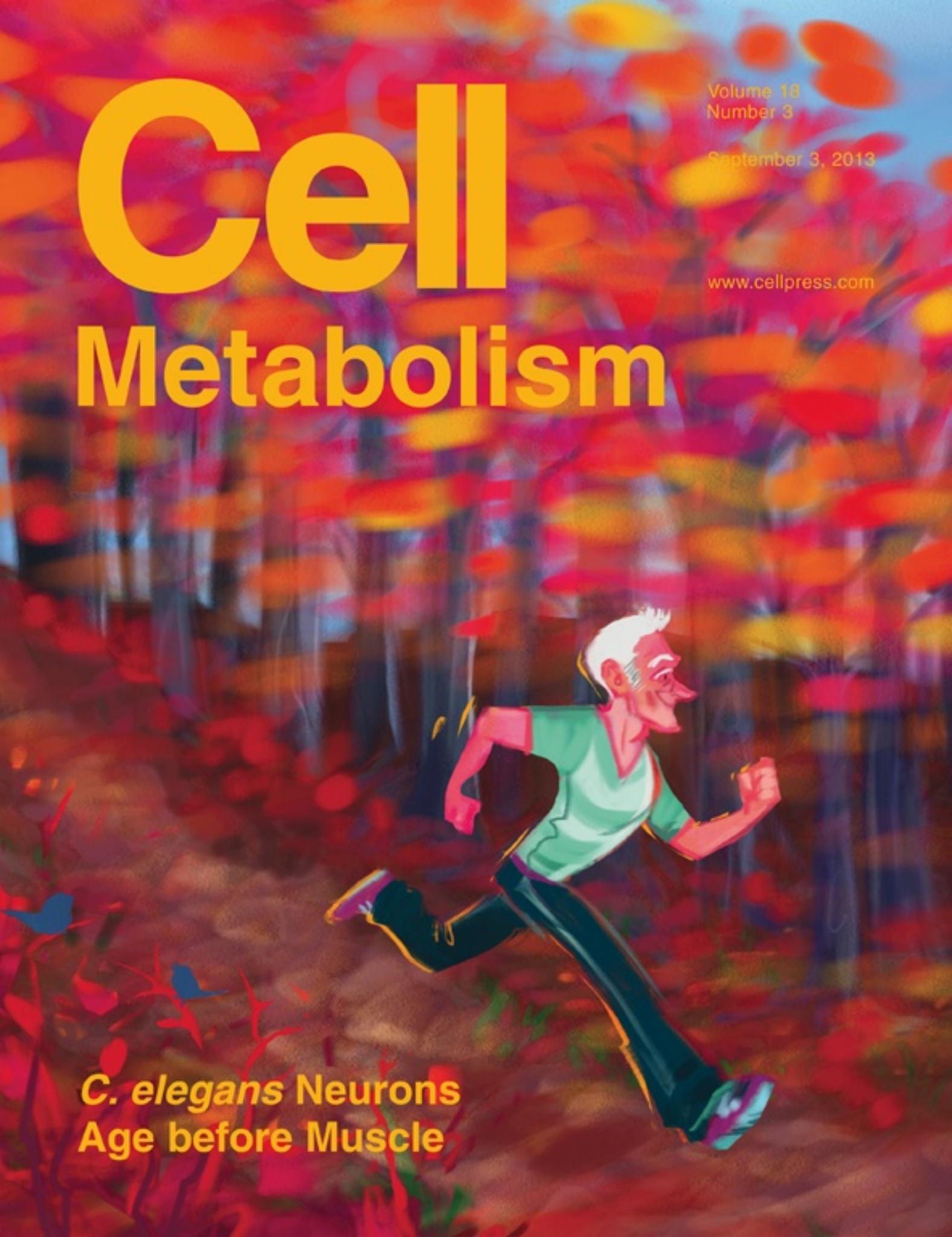

C. elegans Neurons Age before Muscle

Cell Metabolism
Article

Functional Aging in the Nervous System Contributes to Age-Dependent Motor Activity Decline in *C. elegans*

Jie Liu,[1] Bi Zhang,[1,4] Haoyun Lei,[1,4] Zhaoyang Feng,[5] Jianfeng Liu,[4] Ao-Lin Hsu,[2,3] and X.Z. Shawn Xu[1,2,*]
[1]Life Sciences Institute
[2]Department of Molecular and Integrative Physiology
[3]Department of Internal Medicine and Division of Geriatric and Palliative Medicine
University of Michigan, Ann Arbor, MI 48109, USA
[4]College of Life Science and Technology, Huazhong University of Science and Technology, Wuhan, Hubei 430074, China
[5]Department of Pharmacology, Case Western Reserve University, Cleveland, OH 44106, USA
*Correspondence: shawnxu@umich.edu
http://dx.doi.org/10.1016/j.cmet.2013.08.007

SUMMARY

Aging is characterized by a progressive decline in multiple physiological functions (i.e., functional aging). As animals age, they exhibit a gradual loss in motor activity, but the underlying mechanisms remain unclear. Here we approach this question in *C. elegans* by functionally characterizing its aging nervous system and muscles. We find that motor neurons exhibit a progressive functional decline, beginning in early life. Surprisingly, body-wall muscles, which were previously thought to undergo functional aging, do not manifest such a decline until mid-late life. Notably, motor neurons first develop a deficit in synaptic vesicle fusion followed by that in quantal size and vesicle docking/priming, revealing specific functional deteriorations in synaptic transmission. Pharmacological stimulation of synaptic transmission can improve motor activity in aged animals. These results uncover a critical role for the nervous system in age-dependent motor activity decline in *C. elegans* and provide insights into how functional aging occurs in this organism.

INTRODUCTION

Much of the current effort in aging research has been directed to investigating the mechanisms underlying life span regulation. This has greatly advanced our understanding of how genes and environment control life span, particularly in various model organisms (Kenyon, 2010). Nevertheless, it should be noted that aging is in fact characterized by gradual, progressive declines in physiological functions of multiple tissues (i.e., functional aging), which ultimately lead to death (Wolkow, 2006). Yet, the mechanisms underlying functional aging remain largely elusive.

Motor activity decline represents one of the most prominent physiological declines in aging animals and humans. For example, in the nematode *C. elegans*, an organism commonly used as a model for aging research, it was reported in the 1970s that aging worms exhibit a decline in motor activity and that old worms are less active than young worms (Hosono, 1978). This phenomenon has subsequently been noted in many other studies (Dillin et al., 2002; Glenn et al., 2004; Herndon et al., 2002; Hosono et al., 1980; Hsu et al., 2009; Huang et al., 2004; Johnson et al., 1988; Kenyon et al., 1993). Motor deficits have also been observed in elderly humans, which represent one of the main risks for injury and mortality (Faulkner et al., 2007; MacIntosh et al., 2006). However, it remains a long-standing mystery as to what triggers the progressive decline in motor functions in aging humans (Faulkner et al., 2007; MacIntosh et al., 2006).

In *C. elegans*, the mechanisms underlying age-dependent motor activity decline also remain unclear and somewhat controversial. One model proposes that such a decline results from muscle frailty rather than a functional deficit in the nervous system (Herndon et al., 2002). This conclusion is based on the finding that muscle cells undergo morphological deterioration known as sarcopenia in old worms (Herndon et al., 2002); in sharp contrast, the overall integrity of the nervous system morphology is found to be well preserved even at the late stage of worm life (Herndon et al., 2002), though these animals undergo a decline in motor behavior and other types of behaviors (Dillin et al., 2002; Hsu et al., 2009; Huang et al., 2004; Kauffman et al., 2010; Murakami et al., 2005). Recent studies, however, report that a subset of neurons in aging animals exhibit mild morphological abnormalities such as extra neuronal branches, and that worms in their late life (day 15) also show morphological deteriorations at synapses (Pan et al., 2011; Tank et al., 2011; Toth et al., 2012). While the functional implications of these observations are unclear, it indicates that the nervous system undergoes age-related changes at least at the morphological level, suggesting a role for the nervous system in functional aging.

The controversy partly results from the lack of a systematical evaluation of the functional status of the nervous system and muscles throughout life span. Previous studies have largely focused on characterizing the morphology, rather than the function, of the nervous system and muscles. However, morphological analysis may not reliably predict the functional status of a tissue. As such, direct functional characterizations of the aging nervous system and muscles throughout life span are needed to interrogate their roles in age-dependent motor activity loss.

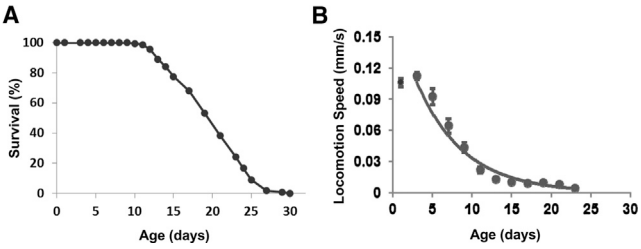

Figure 1. Worms Undergo Progressive Decay in Motor Activity throughout Life Span

(A) Life span curve (Kaplan-Meier test) of N2 worms. Mean life span is 20.2 ± 0.4 (SEM) days. n = 156/173.

(B) Progressive decay in the speed of spontaneous locomotion behavior in aging N2 worms. Worms displayed a progressive decline in locomotion speed beginning in early life. This can be best fit by first-order exponential decay. Error bars represent SD.

See also Figure S1.

One challenge, however, lies in the relative difficulty in assessing the functional status of these tissues in *C. elegans*. Worm neurons and muscles are relatively fragile and small compared to those in insects and mammals (Kang et al., 2010; Waterston, 1988). This poses a technical and logistical challenge to large scales of functional analysis throughout life span, particularly to those involving electrophysiological recording, one of the most frequently used approaches in neurophysiology.

In the current study, we performed a functional analysis of the aging nervous system and muscles in *C. elegans* throughout life span by patch-clamp recordings. We find that despite the preservation of their overall integrity in morphology, motor neurons undergo a progressive decline in function, beginning in early life. Surprisingly, no such functional decline is observed in body-wall muscles in early-mid life, though these muscles functionally deteriorate at mid-late age. We further demonstrated that motor neurons first exhibit a deficit in synaptic vesicle fusion in early life, which is followed by a defect in quantal size and synaptic vesicle docking/priming at later ages. This identifies specific functional deficits in synaptic transmission and also reveals a sequence of events that occur in nervous system aging. Pharmacological interventions that potentiate synaptic transmission of the aging nervous system can improve motor functions in aged animals. Mutations in *daf-2* that extend life span reduce the rate of decline in motor activity and in the function of the motor nervous system. These observations unveil a critical role of nervous system aging, suggesting that age-dependent motor activity decay may primarily result from a progressive functional decline in the nervous system at least during the early-mid phase of animal life. Our studies provide insights into how functional tissue aging may occur in a popular genetic model organism, and how pharmacological and genetic interventions may help reduce the rate of such functional aging.

RESULTS

Aging Worms Gradually Lose Motor Activity, Beginning in Early Life

The N2 wild-type strain has a mean adult life span of approximately 3 weeks (20–21 days) in our hands (Figure 1A). For simplicity, we artificially divided their adult life span into three phases: early life (week 1; day 1–7 adulthood), mid life (week 2; day 8–14), and late life (after week 2; day 15–). As a first step, we confirmed previous observations that as worms age they gradually develop a deficit in motor activity (Dillin et al., 2002; Glenn et al., 2004; Herndon et al., 2002; Hosono, 1978; Hosono et al., 1980; Hsu et al., 2009; Huang et al., 2004; Johnson et al., 1988). We employed an automated worm-tracking system (worm tracker) to record and quantify locomotion behavior in real time (Feng et al., 2006; Hsu et al., 2009; Li et al., 2006). Consistent with previous reports, we found that though worms display a slight increase in locomotion speed between day 1 and 3, they subsequently develop a gradual loss in locomotion speed, beginning at day 5 (Figure 1B).

Aging Worms Exhibit a Progressive Decline in the Function of the Motor Nervous System, Beginning in Early Life

The question arises as to what mechanisms may underlie this progressive decay in locomotion activity in aging worms. One prominent model is that the observed decay may result from muscle defects, as muscle cells undergo morphological deterioration in old worms; yet, the overall integrity of the nervous system morphology is well preserved even at the very late stage of worm life (Herndon et al., 2002). However, this view cannot explain the fact that wild-type worms exhibit a reduction in motor activity beginning as early as day 5 when there is no sign of morphological deterioration in muscle sarcomeres (Glenn et al., 2004; Herndon et al., 2002) (Figure 1B). Not until mid life can a significant change in muscle morphology be detected (Glenn et al., 2004; Herndon et al., 2002). Thus, morphological deterioration in muscle cells alone cannot account for the observed motor activity decay in aging worms.

Considering that it is the function, rather than the morphological features, of a tissue that ultimately determines its role in a behavior or physiological output, we reasoned that a functional deficit in muscle cells and/or the nervous system may underlie the observed decay in locomotion activity in aging worms particularly in their early life. However, no functional characterization of the motor nervous system or body-wall muscles has been performed on aging worms. Therefore, we decided to use electrophysiological approaches to record the activity of the motor nervous system and body-wall muscles in aging worms every other day throughout their life span.

We focused on neuromuscular junctions (NMJs) in the ventral nerve cord. NMJs are specialized synaptic structures formed by motor neurons and muscles. NMJs in the ventral nerve cord are mainly derived from the ventral cord motor neurons and body-wall muscle cells, the activity of which drives locomotion behavior in worms (Chalfie et al., 1985; White et al., 1986). Presynaptic motor neurons spontaneously release neurotransmitters that open muscle receptor channels at NMJs to elicit postsynaptic currents (PSCs). Such PSCs can be recorded by patching muscle cells under voltage clamp. The frequency of spontaneous PSCs at NMJs measures the frequency of spontaneous neurotransmitter release from presynaptic motor neurons, which largely reflects the spontaneous activity of the motor nervous system in the worm body (Madison et al., 2005; Richmond and Jorgensen, 1999). In humans, the frequency of motor unit

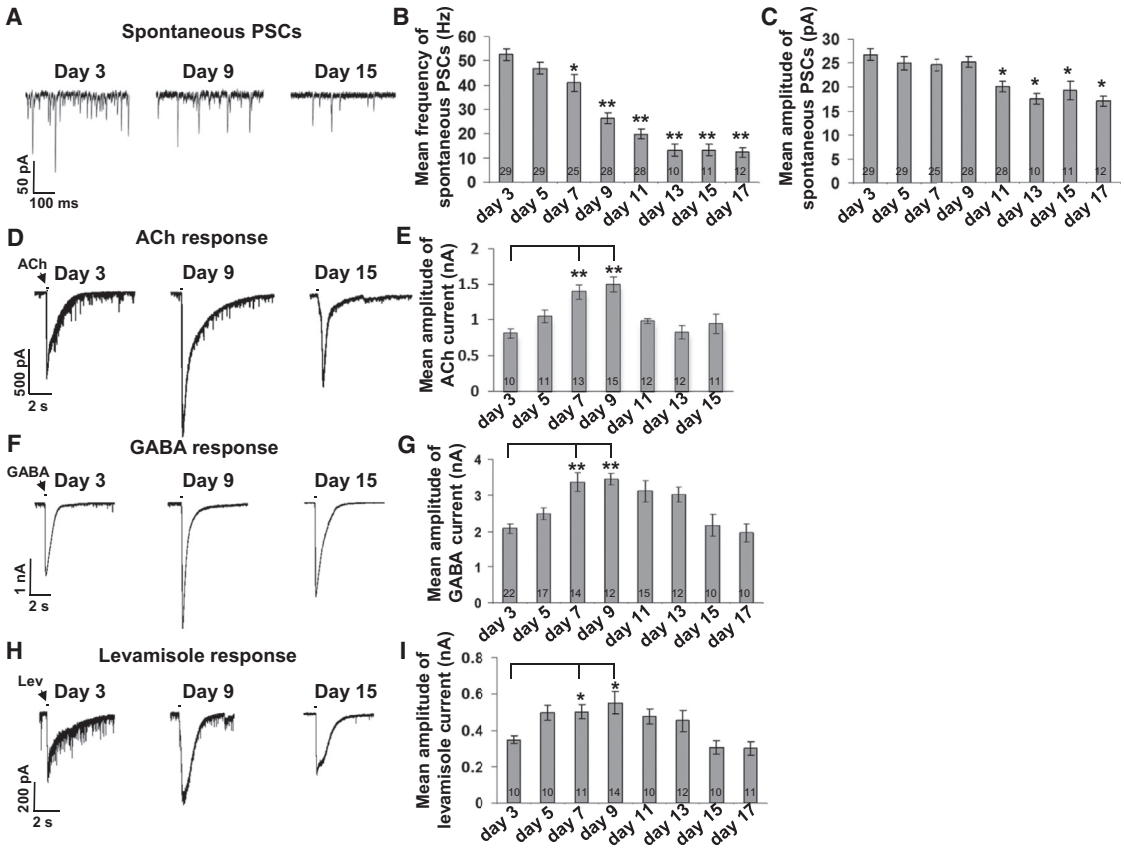

Figure 2. Motor Neurons, but Not Body-Wall Muscle Receptors, Exhibit a Progressive Functional Decline in Wild-Type Worms throughout Life Span

(A) Sample traces of spontaneous PSCs recorded from the ventral cord NMJ of aging wild-type worms. Membrane voltage was clamped at −60 mV during recording.

(B) Bar graph of the frequency of spontaneous PSCs recorded from aging worms throughout life span. *$p < 0.01$; **$p < 0.0001$ (ANOVA with Dunnett test).

(C) Bar graph of the amplitude of spontaneous PSCs recorded from aging worms throughout life span. *$p < 0.005$ (ANOVA with Dunnett test).

(D) Sample traces of body-wall muscle currents evoked by ACh (100 μM) in aging worms.

(E) Bar graph of ACh-evoked currents in body-wall muscle cells of aging worms. **$p < 0.0001$ (ANOVA with Dunnett test).

(F) Sample traces of body-wall muscle currents evoked by GABA (100 μM) in aging worms.

(G) Bar graph of GABA-evoked currents in body-wall muscle cells of aging worms. *$p < 0.005$ (ANOVA with Dunnett test).

(H) Sample traces of body-wall muscle current evoked by levamisole (100 μM) in aging worms.

(I) Bar graph of levamisole-evoked currents in body-wall muscle cells of aging worms. *$p < 0.05$ (ANOVA with Dunnett test).

Sample sizes (n numbers) are embedded in the bars of each graph. All error bars represent SEM.

firings also correlates with the activity of the motor nervous system (MacIntosh et al., 2006).

We recorded spontaneous PSCs at NMJs throughout life span. We found that the frequency of spontaneous PSCs at NMJs began to decline at day 5 and continued until day 17, the last day of recording (Figures 2A and 2B). Interestingly, the trend of this progressive decline in the frequency of spontaneous PSCs paralleled that of progressive decay in locomotion activity (Figure 1B). Between days 1 and 3, there was a slight increase in the frequency of spontaneous PSCs, which is also consistent with behavioral data (Figure 1B and data not shown). These results demonstrate that the motor nervous system undergoes a progressive decline in function during aging, suggesting that this functional decline (i.e., nervous system aging) contributes to the observed progressive decay in locomotion activity in aging worms.

Body-Wall Muscle Receptors Are Functional in Early-Mid Life

Do body-wall muscles also exhibit a similar functional decline in aging worms? To address this question, as a first step we analyzed the amplitude of spontaneous PSCs at NMJs. Unlike the frequency of spontaneous PSCs, the amplitude of these PSCs is affected by the function of both muscle receptors and motor neurons (Madison et al., 2005; Richmond and Jorgensen, 1999). Surprisingly, the amplitude of spontaneous PSCs did not display a significant change until mid life (day 11) (Figure 2C), suggesting that there is no significant decline in the function of body-wall muscle receptors in early-mid life (until day 11).

To provide additional evidence, we directly recorded the activity of muscle receptor channels every other day in aging worms by applying their ligand toward the recorded muscle cell. Two major types of muscle receptor channels are expressed in

body-wall muscles that act to drive muscle contraction and relaxation: the excitatory nicotinic acetylcholine receptors (nAChRs) and inhibitory GABA receptors (Richmond and Jorgensen, 1999). Much to our surprise, the amplitude of ACh- and GABA-evoked muscle currents exhibited a progressive increase rather than a decrease in aging worms, peaking at day 9 (Figures 2D–2G). Though the amplitude of both types of currents began to decline at day 11, it remained higher or comparable to that recorded at day 3 (Figures 3D–3G), indicating a lack of a deficit in muscle receptor functions even in old worms. A similar phenomenon was also observed with muscle currents evoked by the nAChR agonist levamisole (Figures 2H and 2I). Though unexpected, the increase in the amplitude of ACh-, GABA-, and levamisole-evoked muscle currents during days 3–9 might simply reflect a compensatory effect in body-wall muscle cells in response to a reduction in synaptic input from their presynaptic motor neurons (i.e., presynaptic neurotransmitter release) in aging worms. A related phenomenon, though under a different physiological context, has also been reported in other organisms, such as *Drosophila* (Davis and Goodman, 1998). These results provide additional evidence that muscle receptors are functional in early-mid life.

It should be noted that the observed increase in the amplitude of ligand-evoked muscle receptor currents between day 3 and day 9 does not necessarily indicate an increase in the amount of postsynaptic muscle receptors present at NMJs. This is because the amplitude of PSCs remained relatively stable during this time window (Figure 2C). While the amplitude of PSCs correlates with the amount of functional muscle receptors present at synaptic (NMJ) sites under certain circumstances, the amplitude of ligand-evoked muscle currents does not. Instead, the latter largely reflects the overall amount of functional muscle receptors in the entire plasma membrane of muscle cells, including those localized at synaptic (NMJ) as well as nonsynaptic (non-NMJ) sites. Thus, the observed increase in the amplitude of ligand-evoked muscle currents during early-mid life (days 3–9) likely arose from an accumulation of more functional muscle receptors at nonsynaptic (non-NMJ) sites of the plasma membrane of muscle cells. As the amplitude of PSCs is affected by both motor neurons and muscles, we are unable to determine whether the slight decrease in this parameter in mid-late life (day 11 and beyond) resulted from a deficit from neurons or muscles. Nevertheless, our results provide strong evidence that muscle receptors are functional at least up to mid age, suggesting that body-wall muscles do not play a major role in motor activity decay in aging worms at least during their early-mid life.

Mutations in *daf-2* that Extend Life Span Reduce the Rate of Functional Decline in the Motor Nervous System

Insulin/IGF-1-like signaling represents the best characterized genetic pathway for life span regulation. Mutant worms deficient in the insulin/IGF-1-like receptor gene *daf-2* are not only long lived but also appear healthier than wild-type worms at the same age (Kenyon et al., 1993). Indeed, as previously reported (Hsu et al., 2009; Kenyon et al., 1993), *daf-2* worms exhibited a reduced rate of decay in motor activity throughout life span in comparison to wild-type (Figures 3J and 3L and see Figure S1 online).

The observation that *daf-2* mutations reduced the rate of motor activity decay in aging worms raises the question as to what physiological mechanisms may contribute to this healthspan-extending effect mediated by *daf-2*. To address this question, we recorded the NMJs of aging *daf-2* worms throughout their life span by patch clamping. Both *daf-2(e1370)* and *daf-2(e1368)* animals were examined every 4 days until day 27 and day 23, respectively (Figure 3 and Figure S2). As was the case with wild-type worms, the frequency of spontaneous PSCs in both *daf-2* mutants exhibited a progressive decline with age (Figures 3A and 3B; Figures S2A and S2B); however, the rate of this decline was much slower in *daf-2* worms than that in wild-type worms (Figures 3K and 3L). In contrast, no significant decline in the amplitude of spontaneous PSCs was observed in *daf-2(e1370)* or *daf-2(e1368)* aging worms up to day 27 (Figure 3C and Figure S2C), indicative of a lack of functional deficits in muscle receptors of these worms up to this age. A similar phenomenon was also found with ACh-, GABA-, and levamisole-evoked muscle currents in these worms (Figures 3D–3I; Figures S2D–S2I). These results provide further evidence that muscle receptors do not undergo age-dependent functional decline spanning early-to-mid life, and suggest that *daf-2* mutations may reduce the rate of motor activity decay in aging animals primarily by slowing down the rate of functional decline in the nervous system.

No Significant Deficit Is Detected in the Contraction of Body-Wall Muscles in Early-Mid Life

It might be argued that, though muscle receptors are clearly functional in aging worms at least in their early-mid life, muscle cells might nevertheless possess a deficit in initiating contraction in response to activation of muscle receptors. To address this question, we challenged worms at different ages with varying concentrations of levamisole. Levamisole is a potent nAChR agonist commonly used to induce contraction of body-wall muscles in worms (Lackner et al., 1999); as a result, the worm body shortens progressively. We monitored the contraction of the worm body in response to levamisole treatment in real time using our automated worm-tracking system (Feng et al., 2006; Hsu et al., 2009; Li et al., 2006). In doing so, we were able to quantify both the rate and the extent of body contraction in response to activation of muscle receptors.

We focused on day 3, 9, and 15 worms, with each representing early, mid, and late life, respectively. We found that day 9 worms did not display a significant deficit in the rate or extent of body contraction induced by the muscle agonist levamisole when compared to day 3 worms (Figure 4). In fact, day 9 worms showed a significant increase in the extent of body contraction triggered by levamisole at high concentrations (Figures 4A, 4B, and 4E). Nevertheless, the rate of body contraction was reduced in day 15 worms (Figures 4A, 4C, and 4D). It should be emphasized that these results are remarkably in line with our electrophysiological data that also revealed an increase in the amplitude of muscle receptor currents in early-mid life (Figures 2D–2I). These observations suggest that though worms developed a functional deficit in body-wall muscles in mid-late life (day 15), there seemed to be no significant decline in the function of body-wall muscles at the early-mid phase of life, a period during which worms already exhibited a substantial decay in locomotion activity (Figure 1B). Taken together, though motor deficits observed in worms in their mid-late life may be contributed

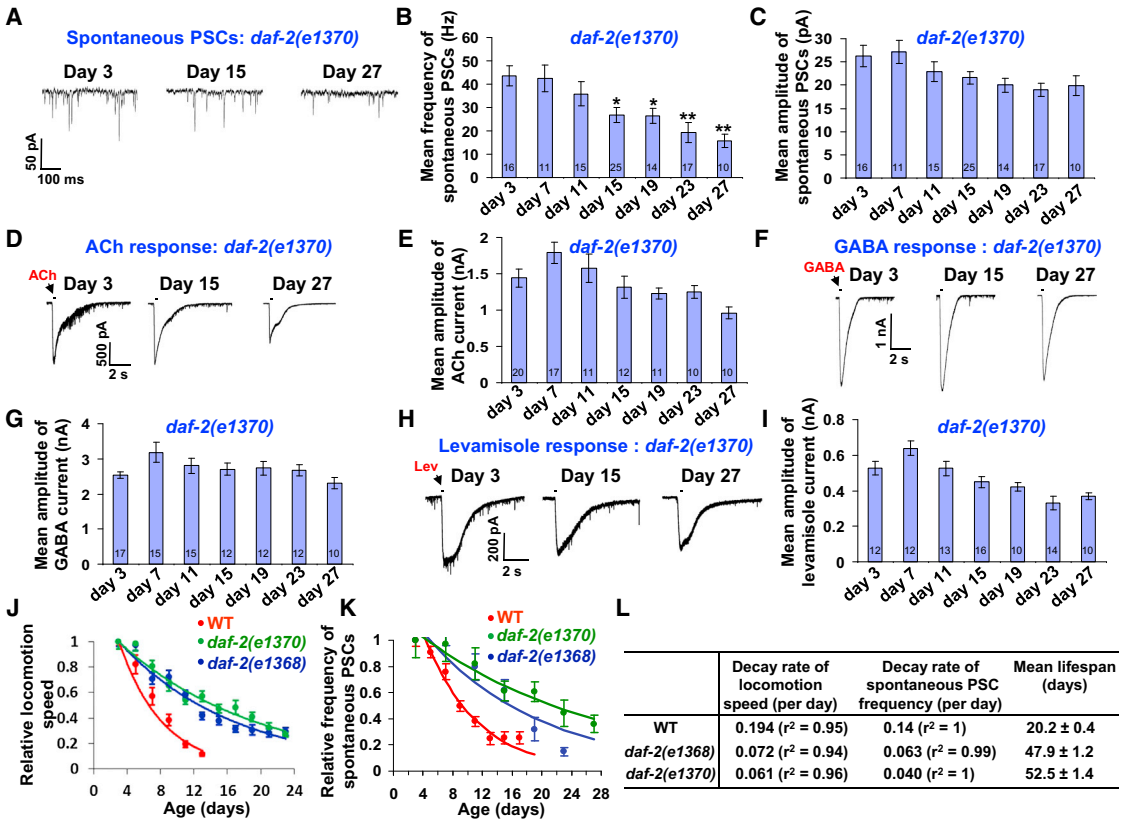

L

	Decay rate of locomotion speed (per day)	Decay rate of spontaneous PSC frequency (per day)	Mean lifespan (days)
WT	0.194 (r^2 = 0.95)	0.14 (r^2 = 1)	20.2 ± 0.4
daf-2(e1368)	0.072 (r^2 = 0.94)	0.063 (r^2 = 0.99)	47.9 ± 1.2
daf-2(e1370)	0.061 (r^2 = 0.96)	0.040 (r^2 = 1)	52.5 ± 1.4

Figure 3. *daf-2(e1370)* Mutation Reduces the Rate of Functional Decline in the Motor Nervous System of Aging Worms

(A) Sample traces of spontaneous PSCs recorded from the ventral cord NMJ of aging *daf-2(e1370)* worms. Membrane voltage was clamped at −60 mV during recording. See Figure S2 for the recording data of *daf-2(e1368)* worms.

(B) Bar graph of the frequency of spontaneous PSCs recorded from aging *daf-2(e1370)* worms throughout life span. *$p < 0.05$; **$p < 0.0005$ (ANOVA with Dunnett test).

(C) Bar graph of the amplitude of spontaneous PSCs recorded from aging worms throughout life span. Error bars represent SEM.

(D) Sample traces of body-wall muscle currents evoked by ACh (100 μM) in aging worms.

(E) Bar graph of ACh-evoked currents in body-wall muscle cells of aging worms. Error bars represent SEM.

(F) Sample traces of body-wall muscle currents evoked by GABA (100 μM) in aging worms.

(G) Bar graph of GABA-evoked currents in body-wall muscle cells of aging worms. Error bars represent SEM.

(H) Sample traces of body-wall muscle currents evoked by levamisole (100 μM) in aging worms.

(I) Bar graph of levamisole-evoked currents in body-wall muscle cells of aging worms. Error bars represent SEM.

(J) The rate of progressive decay in locomotion speed is greatly reduced in aging *daf-2(e1370)* and *daf-2(e1368)* worms. The relative locomotion speed of wild-type (N2) and *daf-2* mutants is plotted as a function of age. The plots can be best fitted by first-order exponential decay, and the rate of decay in each strain was calculated and shown in (L). Error bars represent SD.

(K) The rate of progressive decay in the frequency of spontaneous PSCs at NMJs is greatly reduced in aging *daf-2(e1370)* and *daf-2(e1368)* worms. The relative frequency of spontaneous PSCs of wild-type (N2) and *daf-2* mutants is plotted as a function of age. The plots can be best fitted by first-order exponential decay, and the rate of decay in each strain was calculated and shown in (L). Error bars represent SD.

(L) Table summarizing data in (J) and (K).

Sample sizes (n numbers) are embedded in the bars of each graph. See also Figure S2.

by functional defects in both the nervous system and body-wall muscles, our studies suggest that at the early-mid stage of life, progressive motor activity decay may primarily result from a progressive functional decline in the nervous system.

Motor Neurons First Develop a Deficit in Synaptic Vesicle Fusion Followed by that in Quantal Size and Synaptic Vesicle Docking/Priming

Having demonstrated that motor neurons, rather than body-wall muscles, develop a deficit in early life, we next sought to investigate the underlying mechanisms. The finding that the frequency of spontaneous PSCs decreases with age unveils a functional deficit in synaptic release from motor neurons in aged animals. However, this observation does not provide insights into how synaptic release in motor neurons becomes compromised during aging. Synaptic release from neurons (exocytosis) is a multistep process, including but not limited to neurotransmitter uploading to synaptic vesicles, vesicle docking/priming, and vesicle fusion (Figure 5A) (Südhof and Rizo, 2011). A deficit in any of these steps would lead to a reduction in synaptic release.

To ascertain at which step synaptic release is first compromised in aging motor neurons in early life, we performed additional tests. We first recorded evoked PSCs at NMJs by stimulating the ventral nerve cord with an electrode. This assay

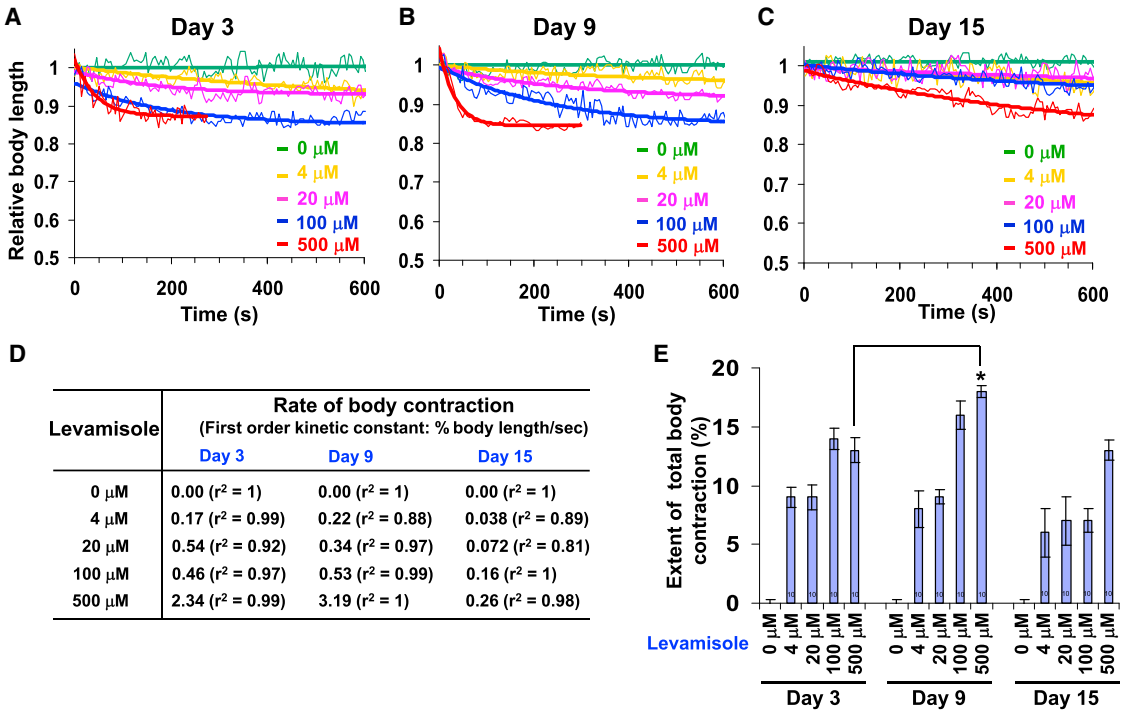

D

Levamisole	Rate of body contraction (First order kinetic constant: % body length/sec)		
	Day 3	Day 9	Day 15
0 μM	0.00 (r^2 = 1)	0.00 (r^2 = 1)	0.00 (r^2 = 1)
4 μM	0.17 (r^2 = 0.99)	0.22 (r^2 = 0.88)	0.038 (r^2 = 0.89)
20 μM	0.54 (r^2 = 0.92)	0.34 (r^2 = 0.97)	0.072 (r^2 = 0.81)
100 μM	0.46 (r^2 = 0.97)	0.53 (r^2 = 0.99)	0.16 (r^2 = 1)
500 μM	2.34 (r^2 = 0.99)	3.19 (r^2 = 1)	0.26 (r^2 = 0.98)

Figure 4. Quantification of the Rate and Extent of Body Contraction in Response to Activation of Muscle Receptors in Aging Worms

(A) Time course of body contraction of day 3 worms in response to different concentrations of levamisole recorded by an automated worm-tracking system. The worm body shortened progressively as a result of body-wall muscle contraction. The process can be best fitted by first-order exponential decay. The thick line running through each trace is the fitting line. Each trace represents data averaged from 10 worms. Levamisole concentrations are indicated.

(B and C) Day 9 and day 15 worms, respectively.

(D) Quantification of the rate of body contraction induced by levamisole. As shown in (A)–(C), the process can be best fitted by first-order exponential decay, and the rate of contraction can be described by the equation $\Delta L / \Delta t = -k * L$, where L denotes the body length of the animal at a given time, t denotes time, and k is a constant. The kinetic constant k is thus used to quantify the rate of body contraction.

(E) Quantification of the extent of body contraction induced by different concentrations of levamisole. The total body contraction during the incubation time was quantified. Quantification of day 3 and day 9 worms treated with 500 μM of levamisole was based on the first 5 min of data, as these worms reached maximal contraction usually within the first 5 min. Error bars represent SEM. *p < 0.01 (t test). Sample sizes (n numbers) are embedded in the bars of the graph.

allows one to interrogate how robustly presynaptic neurons release neurotransmitters in response to nerve impulses (Richmond et al., 1999). As was the case with spontaneous PSCs, evoked PSCs also exhibited a progressive decline, beginning at day 5 in early life (Figures 5B and 5C). This provides further evidence that synaptic transmission at NMJs develops a deficit in early life.

Because postsynaptic muscle receptors remain functionally normal at this early age, the deficit detected in evoked PSCs apparently arose from a reduction in synaptic release from presynaptic motor neurons. In other words, some step(s) in synaptic release from motor neurons must be compromised in early life. To identify such a step, we first examined quantal size. Synaptic release is quantal in nature (Del Castillo and Katz, 1954). Quantal size can be represented by the postsynaptic response to the neurotransmitter released by a single synaptic vesicle from the presynaptic neuron (Del Castillo and Katz, 1954). This parameter is affected by both the amount of neurotransmitter released from synaptic vesicles and the function of postsynaptic muscle receptors present at NMJs. This parameter would correlate with the average amount of neurotransmitters uploaded to individual synaptic vesicles in presynaptic neurons, providing that postsynaptic receptors remain functionally normal. As the function of postsynaptic muscle receptors remained relatively stable at this age (at least up to day 9), a decrease in this parameter in early life would suggest a deficit in the amount of neurotransmitters uploaded to synaptic vesicles. If so, such a deficit would contribute to the observed reduction in evoked PSCs. However, we detected no significant deficit in quantal size until mid life (day 11 and beyond) (Figure 5D). This coincides with the onset of the observed deficit in the amplitude of spontaneous PSCs (Figure 2C). A lack of a deficit in quantal size in early life, therefore, indicates that another step (e.g., vesicle docking/priming and vesicle fusion) in synaptic exocytosis must be compromised at this stage of life.

To distinguish whether synaptic vesicle docking/priming or fusion becomes defective in early life, we quantified the amount of synaptic vesicles docked/primed at nerve terminals. To do so, we measured the size of the readily releasable pool (RRP) by recording PSCs at NMJs in response to hypertonic solutions (sucrose), a parameter that is commonly used to represent the amount of synaptic vesicles docked/primed at nerve terminals (Südhof and Rizo, 2011). Surprisingly, the RRP size remained relatively stable throughout the early-to-mid

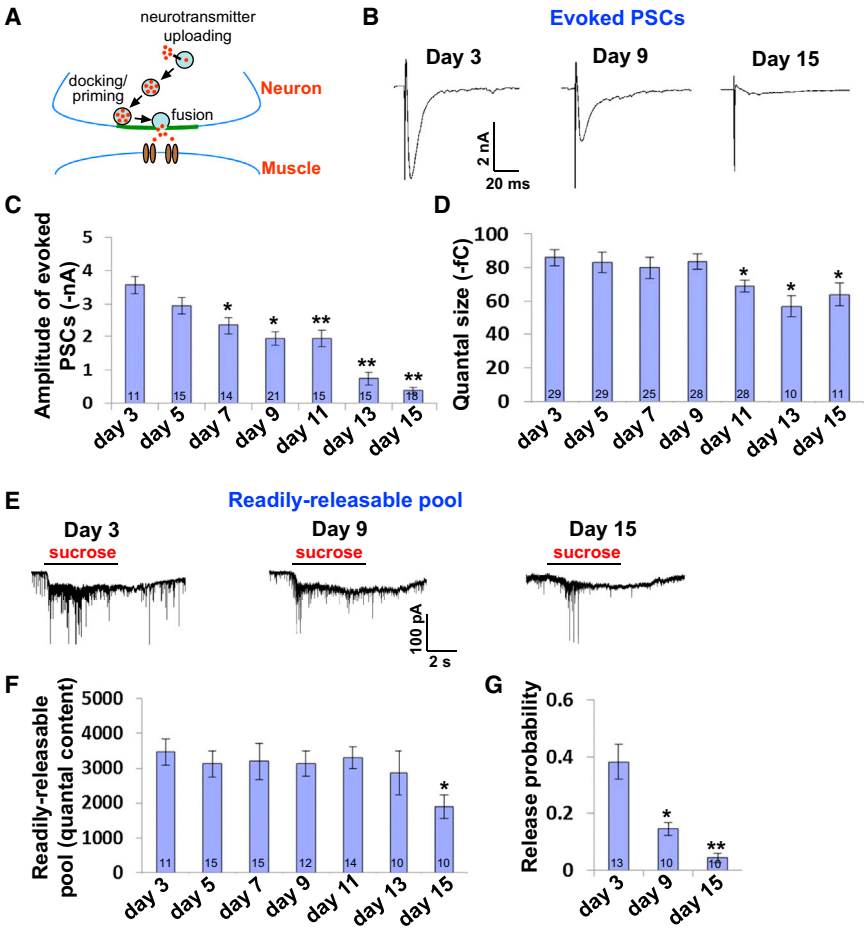

Figure 5. Motor Neurons First Develop a Deficit in Synaptic Vesicle Fusion Followed by that in Quantal Size and Synaptic Vesicle Docking/Priming

(A) A simplified view of synaptic exocytosis. Circles in the neuron denote synaptic vesicles, while ovals in the muscle represent postsynaptic receptors. Dots in red within synaptic vesicles denote neurotransmitters. The thick line in green depicts the active zone at the presynaptic terminal.

(B) Sample traces of evoked PSCs recorded from the ventral cord NMJ of aging wild-type worms.

(C) Bar graph summarizing the amplitude of evoked PSCs throughout life span. *$p < 0.01$; **$p < 0.0001$ (ANOVA with Dunnett test).

(D) Quantal size. *$p < 0.005$ (ANOVA with Dunnett test).

(E) Sample traces of hypertonic sucrose solution-evoked PSCs in aging wild-type worms.

(F) The size of readily releasable pool represented by the number of vesicles released by perfusion of hypertonic sucrose solution. *$p < 0.01$ (ANOVA with Dunnett test).

(G) The relative release probability. The same animal was recorded for hypertonic solution-triggered PSCs followed by evoked PSCs. Prior to recording evoked PSCs, a 3 min recovery was allowed. We have done control experiments showing that such an interval was sufficient to permit a full recovery. The relative release probability was estimated by dividing the total number of quantum released by hypertonic solution with that measured in evoked PSCs. *$p < 0.03$; **$p < 0.001$ (ANOVA with Dunnett test).

Sample sizes (n numbers) are embedded in the bars of each graph. All error bars represent SEM.

life of the animal, a time window during which motor neurons already manifested a deficit in synaptic release (Figures 5E and 5F). Apparently, though synaptic vesicles contain a normal amount of neurotransmitters and can efficiently dock and prime in early life, they become less efficient in fusing with motor neuron terminals. Thus, the events upstream of synaptic vesicle fusion (e.g., neurotransmitter uploading and vesicle docking/priming) do not appear to be defective in early life. This identifies synaptic vesicle fusion as an early event in nervous system aging.

It should be noted that though RRP and quantal size did not exhibit a deficit in early life, these two parameters did deteriorate at later ages. Specifically, quantal size began to decrease at day 11 followed by RRP at day 15 (Figures 5D–5F). Thus, vesicle docking/priming (represented by the size of RRP) appears to develop a deficit in late life. Nevertheless, as quantal size is not just affected by the amount of neurotransmitter released from synaptic vesicles (the function of postsynaptic muscle receptors also contributes), we are unable to determine whether neurotransmitter uploading becomes defective beyond early life.

We further directly quantified the relative release probability of synaptic vesicles in motor neurons by measuring both evoked PSCs and RRP in the same animal. Given that this assay is a lot more technically challenging, we focused on day 3, 9, and 15 worms. Indeed, the relative release probability gradually decreased with age (Figure 5G). Taken together, our results demonstrate that motor neurons first develop a deficit in synaptic vesicle fusion in early life, which is followed by a defect in quantal size and vesicle docking/priming at later ages. This identifies specific functional deficits in synaptic transmission and also reveals a sequence of events that occur in nervous system aging.

Effects of *daf-2* Mutation on Synaptic Transmission in Aging Motor Neurons

We then characterized how insulin/IGF-1-like signaling affects the specific steps of synaptic transmission in aging motor neurons. Similar to that observed with spontaneous PSCs, *daf-2* mutant worms showed a gradual decline in the amplitude of evoked PSCs (Figures 6A and 6B); however, the rate of the decline was much slower than that found in wild-type worms (Figure 6C). As was the case with wild-type, both the quantal size and RRP size remained relatively stable in *daf-2* worms up to day 27 (Figures 6D and 6E and Figure S3). Similarly, the relative release probability of synaptic vesicles also gradually decreased with age but at a lower rate than that in wild-type worms (Figure 6F). Thus, a reduction in insulin/IGF-1-like signaling slows down the rate of the functional decline in synaptic transmission.

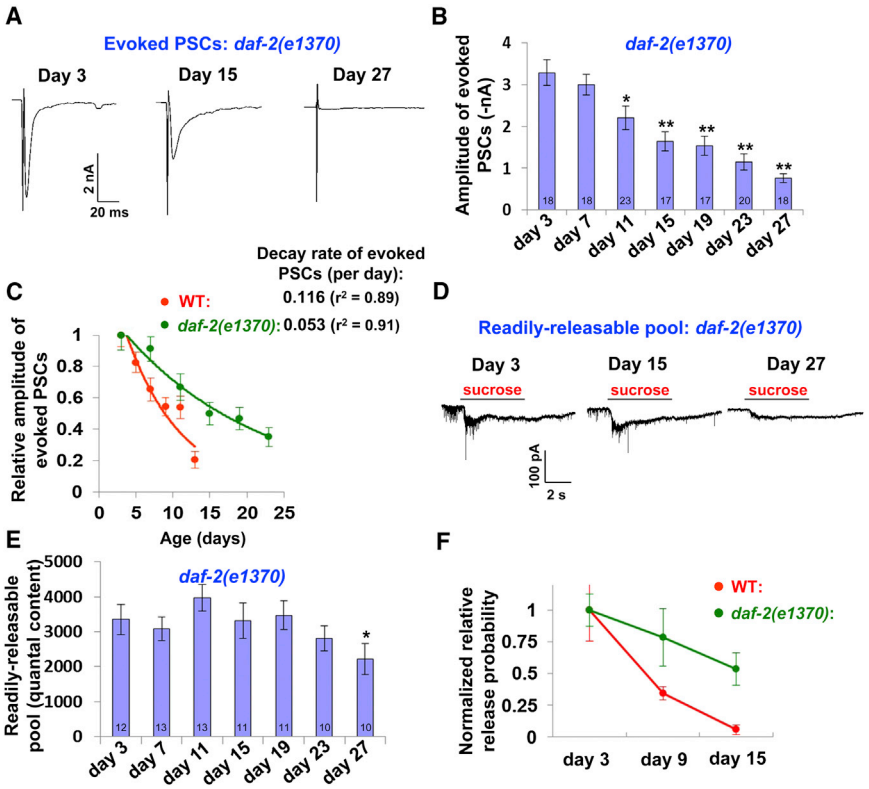

Figure 6. Effects of *daf-2* Mutation on Synaptic Transmission in Aging Motor Neurons

(A) Sample traces of evoked PSCs recorded from the ventral cord NMJ of aging *daf-2(e1370)* worms.

(B) Bar graph summarizing the amplitude of evoked PSCs throughout the life span of *daf-2(e1370)* worms. *$p < 0.01$; **$p < 0.0001$ (ANOVA with Dunnett test). Error bars represent SEM.

(C) The rate of progressive decay in evoked PSCs is reduced in aging *daf-2(e1370)* worms. The relative amplitude of evoked PSCs of wild-type (N2) and *daf-2* mutant worms is plotted as a function of age. The plots can be best fitted by first-order exponential decay, and the rate of decay was calculated and shown. Error bars represent SD.

(D) Sample traces of hypertonic sucrose solution-evoked PSCs in aging *daf-2(e1370)* worms.

(E) The size of readily releasable pool represented by the number of vesicles released by perfusion of hypertonic sucrose solutions in aging *daf-2(e1370)* worms. *$p < 0.02$ (ANOVA with Dunnett test). Error bars represent SEM.

(F) Normalized relative release probability. Relative release probability in aging *daf-2(e1370)* worms was calculated using the protocol described in the legends of Figure 5G. Relative release probability in both N2 and *daf-2(e1370)* worms was normalized to day 3 worms. Error bars represent SEM. Sample sizes (n numbers) are embedded in the bars of each graph. See also Figure S3.

Pharmacological Stimulation of Synaptic Transmission in the Aging Motor Nervous System Improves Motor Activity in Aged Worms

We then sought to provide additional evidence. We reasoned that if the functional decline in the aging motor nervous system leads to motor activity decay, then stimulating the activity of the motor nervous system should stimulate motor activity in aged worms. Previous work using behavioral assays suggests that arecoline, a muscarinic AChR agonist, can specifically potentiate neurotransmitter release by promoting synaptic vesicle fusion but has no effect on the activity of muscle receptors at NMJs in the ventral nerve cord (Lackner et al., 1999). We thus wondered if arecoline can stimulate locomotion activity in aged worms. As a first step, we examined by whole-cell patch-clamp recording whether arecoline can potentiate synaptic release from motor neurons in the ventral nerve cord. We found that arecoline treatment significantly augmented the frequency, but not the amplitude, of spontaneous PSCs at NMJs in aged worms (Figures 7A–7C), demonstrating that arecoline can promote the activity of motor neurons without having a direct effect on body-wall muscle receptors. Arecoline also had no effect on quantal size (Figure S4A). In addition, arecoline treatment did not significantly alter the amplitude of muscle currents evoked by ACh, GABA, or levamisole (Figures 7D and 7E; Figures S4B and S4C), providing further evidence for the specificity of arecoline in potentiating neuronal activities.

Lastly, we recorded evoked PSCs and found that arecoline promoted evoked PSCs but had no effect on the size of RRP (Figures 7F–7I). Thus, arecoline appears to potentiate the activity of the motor nervous system by specifically stimulating synaptic vesicle fusion.

Having demonstrated that arecoline treatment can potentiate the activity of the motor nervous system by stimulating synaptic transmission, we then tested whether arecoline treatment can improve locomotion activity in aged worms. We found that the speed of locomotion in aged worms treated with arecoline was significantly higher than that of mock-treated worms (Figure 7J; Movie S1, Movie S2, Movie S3, and Movie S4). Arecoline treatment also improved other locomotion parameters in aged worms (Figures S4D–S4H). These results provide additional evidence supporting a role for nervous system aging in age-dependent motor activity decay. They also demonstrate that pharmacological stimulation of the aging nervous system can improve motor functions in aged animals.

DISCUSSION

Aging is characterized by a progressive functional decline in multiple tissues (i.e., functional aging), which is associated with an increased likelihood of death. While recent studies in model organisms have greatly advanced our understanding of life span regulation, much less is known about the mechanisms underlying functional aging. To approach this question, it is necessary to interrogate the functional status of aging tissues throughout life span. In the current study, we performed the first functional characterization of the aging nervous system and muscles in *C. elegans* throughout life span. We uncovered a sequence of events that occur during aging in motor neurons

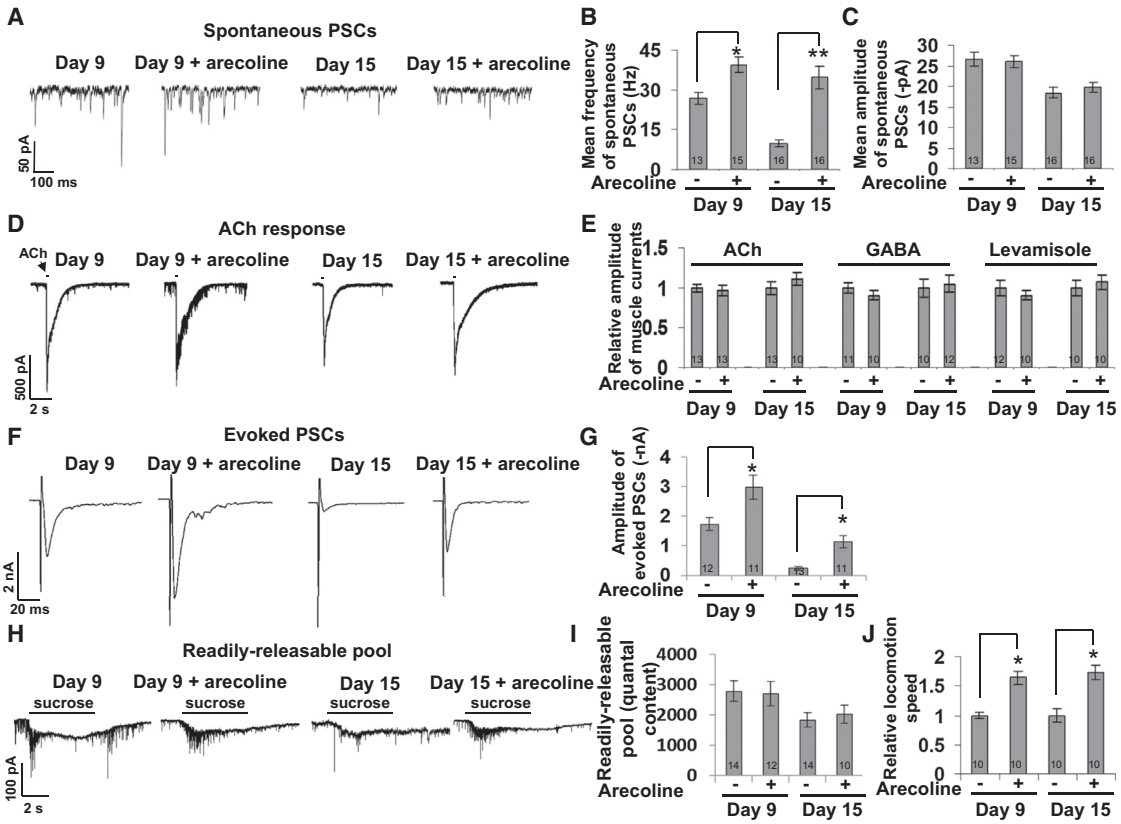

Figure 7. Pharmacological Stimulation of the Motor Nervous System Improves Locomotion Activity in Aged Worms

(A) Sample traces of spontaneous PSCs recorded from the ventral cord NMJ of aged wild-type worms (day 9 and day 15) with or without arecoline treatment. Membrane voltage was clamped at −60 mV during recording.

(B) Frequency of spontaneous PSCs recorded from day 9 and day 15 wild-type worms with or without arecoline treatment. *$p < 0.002$; **$p < 0.0001$ (t test).

(C) Amplitude of spontaneous PSCs. The same sample as in (B) was analyzed.

(D) Sample traces of body-wall muscle currents evoked by ACh in aged wild-type worms with or without arecoline treatment.

(E) Bar graph summarizing body-wall muscle currents evoked by ACh, GABA, and levamisole in aged worms with or without arecoline treatment.

(F and G) Arecoline treatment potentiates evoked PSCs in aged worms. Day 9 and day 15 worms were tested. *$p < 0.01$ (t test).

(H and I) Arecoline treatment has no significant effect on the size of readily releasable pool.

(J) Arecoline treatment potentiates the speed of locomotion in aged worms. Day 9 or day 15 worms were assayed for spontaneous locomotion behavior on plates with or without arecoline. *$p < 0.03$ (t test).

Sample sizes (n numbers) are embedded in the bars of each graph. All error bars represent SEM. See also Figure S4 and Movie S1, Movie S2, Movie S3, and Movie S4.

and body-wall muscles. Our data show that motor neurons first undergo a progressive decline in function, beginning in early life. Body-wall muscles then begin to deteriorate functionally, but not until the mid-late stage of aging. Further analysis reveals that motor neurons first develop a deficit in synaptic vesicle fusion, beginning in early life, which is followed by a defect in quantal size and vesicle docking/priming at later ages. A similar phenomenon may occur in other types of neurons in aging worms. Life span-extending mutations reduce the rate of motor activity decay as well as the rate of functional decline in the aging motor nervous system. Pharmacological stimulation of the aging nervous system can improve motor functions in aged animals. Our studies not only illustrate an example of how functional aging may occur in a genetic model organism but also provide insights into how genetic and pharmacological interventions may help slow down the rate of such functional aging.

We provided multiple lines of evidence supporting the notion that progressive motor activity decay during aging may primarily result from a progressive functional decline in the motor nervous system at least during the early-to-mid phase of life. First, worms exhibit a progressive decline in the function of motor neurons, beginning in early life, and the trend of this decline parallels that of motor activity decay. Second, we did not observe a similar decline in the function of muscle receptors at this age, and muscle contraction also appears to be largely normal up to mid life. Instead, there seems to be an upregulation of the overall activity of muscle receptors in early-to-mid life, probably reflecting a compensatory effect in response to a reduction in synaptic input from motor neurons. Third, life span-extending mutations in *daf-2* reduce the rate of motor activity decay and the rate of functional decline in motor neurons. Lastly, we show that pharmacological stimulation of the aging nervous system can potentiate locomotion activity in aged worms. These

observations together suggest that functional decline in the nervous system is an important mechanism that underlies progressive motor activity decay in aging worms. These results also suggest that nervous system aging may precede muscle aging in worms. As nervous system aging can be detected in early life, this indicates that functional tissue aging in *C. elegans* may begin earlier than previously realized.

Our results do not favor the view that muscle defects underlie motor activity decay in aging worms (Herndon et al., 2002), which is based on morphological characterization, rather than functional evaluation, of worm tissues during aging (Herndon et al., 2002). Our data demonstrate that functional deficits may develop at a time when no notable morphological deteriorations are detected using the assays currently available.

Nevertheless, functional deficits may be accompanied by morphological deteriorations, particularly at relatively late stages of worm life. For example, a recent study detected a reduction in synaptic vesicle density in some unknown head neurons in late life (day 15) (Toth et al., 2012), a stage when motor neurons show a severe functional deficit. Several studies reported a growth of extra branches in some neuronal types in early-mid life, though the functional implications of this observation remain unclear (Pan et al., 2011; Tank et al., 2011; Toth et al., 2012). We also identified a functional deficit in body-wall muscles in late life (day 15), a stage when muscle morphology is severely deteriorated (Herndon et al., 2002). It is not known what triggers the onset of morphological deteriorations in body-wall muscles. One potential mechanism may involve nervous system aging—for example, a reduction in synaptic input received by body-wall muscles from motor neurons. In mammals, denervation leads to muscle atrophy (MacIntosh et al., 2006).

Elderly humans also develop deficits in motor function, which represent one of the main risks for falling that leads to injury and mortality (Faulkner et al., 2007; MacIntosh et al., 2006). Loss of both motor units and muscle fibers is observed during aging, beginning in mid life (i.e., ~50 years old), which is accompanied with a decrease in motor function; however, the mechanisms underlying such a decline are not well understood (Faulkner et al., 2007; MacIntosh et al., 2006). In particular, it remains a long-standing mystery whether this functional decline is triggered by nervous system aging or muscle aging (Faulkner et al., 2007; MacIntosh et al., 2006). Our data suggest that nervous system aging may precede muscle aging in *C. elegans*. Given the high conservation of aging mechanisms between worms and other organisms, our results raise the possibility that a similar phenomenon may occur in mammals.

EXPERIMENTAL PROCEDURES

Quantification of Locomotion Activity, Life Span, and Body Contraction

Locomotion behavior was assayed on NGM plates every other day throughout life span using an automated worm-tracking system (Worm Tracker) described previously (Feng et al., 2006; Li et al., 2006). Briefly, NGM plates were spread with a thin layer of freshly grown OP50 bacteria 5 min prior to tracking. We performed tracking at 20°C under a relative humidity of ~40% with the lid off. The Worm Tracker consists of a stereomicroscope (Zeiss Stemi 2000C) mounted with a digital camera (Cohu 7800) and a digital motion system (Parker Automation) that follows worm movement. A customer-developed software package was used to control the system. Worm images were recorded at 2 Hz for 5 min, and the mean centroid speed of each worm was quantified and displayed in real time. To test the effect of arecoline on locomotion, the animal was first tracked on a drug-free plate. After 4 hr of rest, the same animal was then assayed for locomotion behavior on an arecoline-containing plate (0.2 mM). To allow arecoline to enter the worm to elicit its effect, images from the initial 10 min of tracking were not included for analysis.

To quantify body contraction induced by levamisole, worms were first incubated in drug-free solution (140 mM NaCl, 5 mM KCl, 5 mM $CaCl_2$, 5 mM $MgCl_2$, 11 mM dextrose, and 5 mM HEPES; 330 mOsm; pH adjusted to 7.2 with NaOH) and then in levamisole-containing solution for 10 min. The entire process was recorded by an automated worm-tracking system. The vision data were compressed and stored as a commonly used multimedia file format (AVI), and those frames showing that part of the worm body was out of focus were discarded. Images were thinned, and the length of the worm body was quantified using laboratory-developed software.

Life span analysis was conducted at 20°C as described previously (Kenyon et al., 1993). In all experiments, the first day of adulthood was scored as day 1. Each worm was scored for its viability every day. Worms that crawled off the plate, exploded, or bagged were censored at the time of the event. All statistical analyses were done using the Statistica (StatSoft, Inc.) and Statview 5.01 (SAS) software. In a parallel experiment, 240 worms of each strain were grown on NGM plates (12 per plate), and one animal from each plate (total of 20 plates) was randomly picked (without knowing its movement capability) for analysis of movement behavior using our automated worm-tracking system. This behavioral experiment was repeated in Figure S1.

Electrophysiology

Whole-cell patch-clamp recordings of NMJs were performed under a 60× water immersion lens with an EPC-10 amplifier and the Patchmaster software (HEKA), using a protocol described by Richmond et al. (Richmond and Jorgensen, 1999). Voltages were clamped at −60 mV. Current data were sampled at 5 kHz. Series resistance and membrane capacitance were both compensated. Sixty second recordings of spontaneous PSCs from each worm were analyzed for the frequency and amplitude of spontaneous PSCs using MiniAnalysis (Synaptosoft, Inc.). Muscle receptor ligands and hypertonic sucrose solution were applied using a pressurized perfusion system (ALA Scientific). Evoked PSCs were triggered by a 0.5 ms pulse (25 V) using a stimulating electrode placed in close proximity to the ventral nerve cord. Recording pipettes (4–6 MΩ) were pulled from borosilicate glass and fire polished. The pipette solution contains 120 mM KCl, 20 mM KOH, 4 mM $MgCl_2$, 10 mM HEPES, 0.25 mM $CaCl_2$, 36 mM sucrose, 5 mM EGTA, and 4 mM Na_2ATP (315 mOsm; pH adjusted to 7.2). The bath solution contains 140 mM NaCl, 5 mM KCl, 5 mM $CaCl_2$, 5 mM $MgCl_2$, 11 mM dextrose, and 5 mM HEPES (330 mOsm; pH adjusted to 7.2). Muscle receptor ligands were diluted in bath solution to a final concentration of 100 μM. Hypertonic solution was made by adding sucrose to bath solution to a final concentration of 1 M. Quantal size (net charge transfer per quantum) was estimated by analyzing miniature spontaneous PSC traces. To estimate the RRP size, we quantified the number of vesicles (quantal content) released by 5 s application of hypertonic solution. Quantal content in evoked PSCs was calculated in a similar manner. Basal line release was subtracted. To record the effects of arecoline on NMJ activity, worms were pretreated with arecoline (0.2 mM) for ~10 min and recorded in bath solution containing the same concentration of arecoline.

SUPPLEMENTAL INFORMATION

Supplemental Information includes four figures and four movies and can be found with this article online at http://dx.doi.org/10.1016/j.cmet.2013.08.007.

ACKNOWLEDGMENTS

We thank John Faulkner for advice, Anuj Kumar for critically reading an early version of the manuscript, and Bin Cao and Alex Ward for technical assistance. Some strains were obtained from the Caenorhabditis Genetics Center. This work was supported by the Ministry of Science and Technology of China (2012CB51800 to J.L.), NSFC (31130028 and 31225011 to J.L.), the Program of Introducing Talents of Discipline to the Universities from the Ministry of Education of China (B08029 to J.L.), and grants from the National Institute

on Aging (A.-L.H.), the National Institute of General Medical Sciences (X.Z.S.X.), and the Pew Scholar Program (X.Z.S.X.).

Received: January 11, 2013
Revised: May 30, 2013
Accepted: July 28, 2013
Published: September 3, 2013

REFERENCES

Chalfie, M., Sulston, J.E., White, J.G., Southgate, E., Thomson, J.N., and Brenner, S. (1985). The neural circuit for touch sensitivity in *Caenorhabditis elegans*. J. Neurosci. *5*, 956–964.

Davis, G.W., and Goodman, C.S. (1998). Synapse-specific control of synaptic efficacy at the terminals of a single neuron. Nature *392*, 82–86.

Del Castillo, J., and Katz, B. (1954). Quantal components of the end-plate potential. J. Physiol. *124*, 560–573.

Dillin, A., Hsu, A.L., Arantes-Oliveira, N., Lehrer-Graiwer, J., Hsin, H., Fraser, A.G., Kamath, R.S., Ahringer, J., and Kenyon, C. (2002). Rates of behavior and aging specified by mitochondrial function during development. Science *298*, 2398–2401.

Faulkner, J.A., Larkin, L.M., Claflin, D.R., and Brooks, S.V. (2007). Age-related changes in the structure and function of skeletal muscles. Clin. Exp. Pharmacol. Physiol. *34*, 1091–1096.

Feng, Z., Li, W., Ward, A., Piggott, B.J., Larkspur, E.R., Sternberg, P.W., and Xu, X.Z.S. (2006). A *C. elegans* model of nicotine-dependent behavior: regulation by TRP-family channels. Cell *127*, 621–633.

Glenn, C.F., Chow, D.K., David, L., Cooke, C.A., Gami, M.S., Iser, W.B., Hanselman, K.B., Goldberg, I.G., and Wolkow, C.A. (2004). Behavioral deficits during early stages of aging in *Caenorhabditis elegans* result from locomotory deficits possibly linked to muscle frailty. J. Gerontol. A Biol. Sci. Med. Sci. *59*, 1251–1260.

Herndon, L.A., Schmeissner, P.J., Dudaronek, J.M., Brown, P.A., Listner, K.M., Sakano, Y., Paupard, M.C., Hall, D.H., and Driscoll, M. (2002). Stochastic and genetic factors influence tissue-specific decline in ageing *C. elegans*. Nature *419*, 808–814.

Hosono, R. (1978). Age dependent changes in the behavior of Caenorhabditis elegans on attraction to Escherichia coli. Exp. Gerontol. *13*, 31–36.

Hosono, R., Sato, Y., Aizawa, S.I., and Mitsui, Y. (1980). Age-dependent changes in mobility and separation of the nematode Caenorhabditis elegans. Exp. Gerontol. *15*, 285–289.

Hsu, A.L., Feng, Z., Hsieh, M.Y., and Xu, X.Z. (2009). Identification by machine vision of the rate of motor activity decline as a lifespan predictor in *C. elegans*. Neurobiol. Aging *30*, 1498–1503.

Huang, C., Xiong, C., and Kornfeld, K. (2004). Measurements of age-related changes of physiological processes that predict lifespan of Caenorhabditis elegans. Proc. Natl. Acad. Sci. USA *101*, 8084–8089.

Johnson, T.E., Conley, W.L., and Keller, M.L. (1988). Long-lived lines of Caenorhabditis elegans can be used to establish predictive biomarkers of aging. Exp. Gerontol. *23*, 281–295.

Kang, L., Gao, J., Schafer, W.R., Xie, Z., and Xu, X.Z.S. (2010). C. elegans TRP family protein TRP-4 is a pore-forming subunit of a native mechanotransduction channel. Neuron *67*, 381–391.

Kauffman, A.L., Ashraf, J.M., Corces-Zimmerman, M.R., Landis, J.N., and Murphy, C.T. (2010). Insulin signaling and dietary restriction differentially influence the decline of learning and memory with age. PLoS Biol. *8*, e1000372, http://dx.doi.org/10.1371/journal.pbio.1000372.

Kenyon, C.J. (2010). The genetics of ageing. Nature *464*, 504–512.

Kenyon, C., Chang, J., Gensch, E., Rudner, A., and Tabtiang, R. (1993). A C. elegans mutant that lives twice as long as wild type. Nature *366*, 461–464.

Lackner, M.R., Nurrish, S.J., and Kaplan, J.M. (1999). Facilitation of synaptic transmission by EGL-30 Gqalpha and EGL-8 PLCbeta: DAG binding to UNC-13 is required to stimulate acetylcholine release. Neuron *24*, 335–346.

Li, W., Feng, Z., Sternberg, P.W., and Xu, X.Z.S. (2006). A *C. elegans* stretch receptor neuron revealed by a mechanosensitive TRP channel homologue. Nature *440*, 684–687.

MacIntosh, B.R., Gardiner, P.F., and McComas, A.J. (2006). Skeletal Muscle, Second Edition (Champaign, IL: Human Kinetics).

Madison, J.M., Nurrish, S., and Kaplan, J.M. (2005). UNC-13 interaction with syntaxin is required for synaptic transmission. Curr. Biol. *15*, 2236–2242.

Murakami, H., Bessinger, K., Hellmann, J., and Murakami, S. (2005). Aging-dependent and -independent modulation of associative learning behavior by insulin/insulin-like growth factor-1 signal in Caenorhabditis elegans. J. Neurosci. *25*, 10894–10904.

Pan, C.L., Peng, C.Y., Chen, C.H., and McIntire, S. (2011). Genetic analysis of age-dependent defects of the *Caenorhabditis elegans* touch receptor neurons. Proc. Natl. Acad. Sci. USA *108*, 9274–9279.

Richmond, J.E., and Jorgensen, E.M. (1999). One GABA and two acetylcholine receptors function at the *C. elegans* neuromuscular junction. Nat. Neurosci. *2*, 791–797.

Richmond, J.E., Davis, W.S., and Jorgensen, E.M. (1999). UNC-13 is required for synaptic vesicle fusion in *C. elegans*. Nat. Neurosci. *2*, 959–964.

Südhof, T.C., and Rizo, J. (2011). Synaptic vesicle exocytosis. Cold Spring Harb. Perspect. Biol. *3*, 3.

Tank, E.M., Rodgers, K.E., and Kenyon, C. (2011). Spontaneous age-related neurite branching in Caenorhabditis elegans. J. Neurosci. *31*, 9279–9288.

Toth, M.L., Melentijevic, I., Shah, L., Bhatia, A., Lu, K., Talwar, A., Naji, H., Ibanez-Ventoso, C., Ghose, P., Jevince, A., et al. (2012). Neurite sprouting and synapse deterioration in the aging Caenorhabditis elegans nervous system. J. Neurosci. *32*, 8778–8790.

Waterston, R.H. (1988). Muscle. In The Nematode *Caenorhabditis elegans*The Nematode *Caenorhabditis elegans* (New York: Cold Spring Harbor Laboratory Press), pp. 281–335.

White, J.G., Southgate, E., Thomson, J.N., and Brenner, S. (1986). The structure of the nervous system of the nematode Caenorhabditis elegans. Philos. Trans. R. Soc. Lond. B Biol. Sci. *314*, 1–340.

Wolkow, C.A. (2006). Identifying factors that promote functional aging in Caenorhabditis elegans. Exp. Gerontol. *41*, 1001–1006.

Figure S1

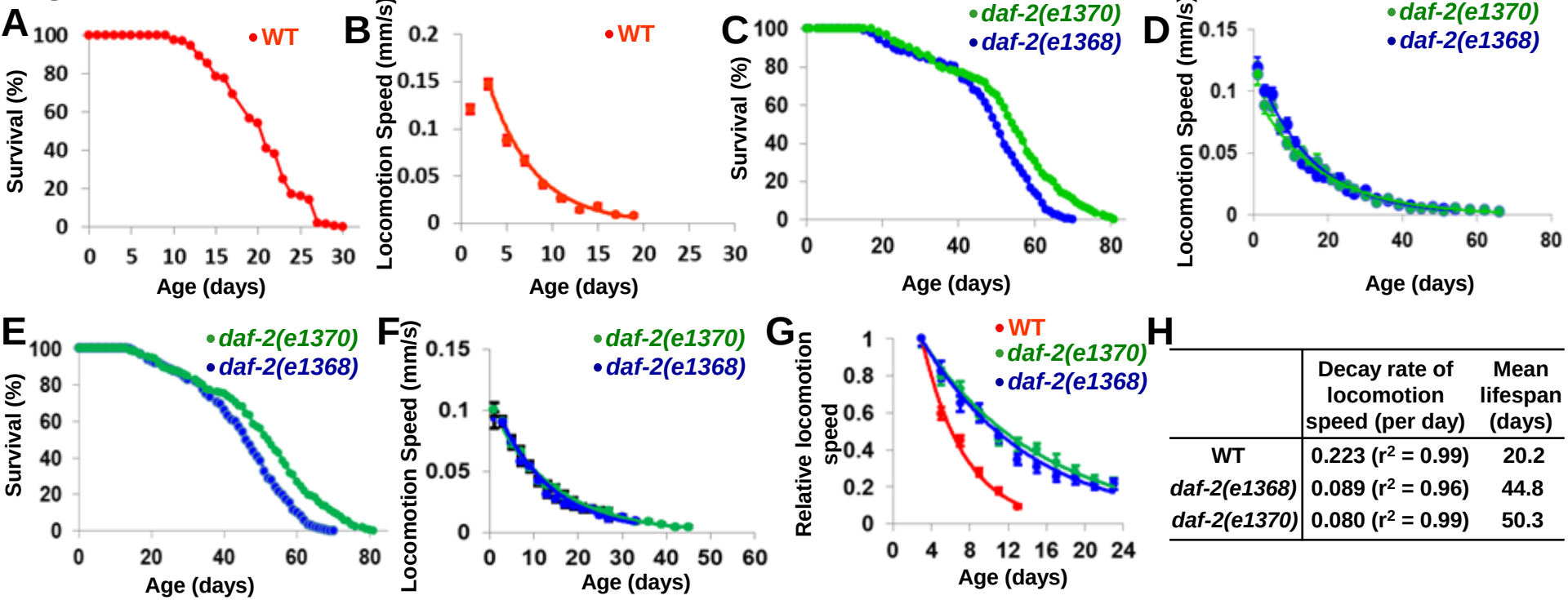

H

	Decay rate of locomotion speed (per day)	Mean lifespan (days)
WT	0.223 (r^2 = 0.99)	20.2
daf-2(e1368)	0.089 (r^2 = 0.96)	44.8
daf-2(e1370)	0.080 (r^2 = 0.99)	50.3

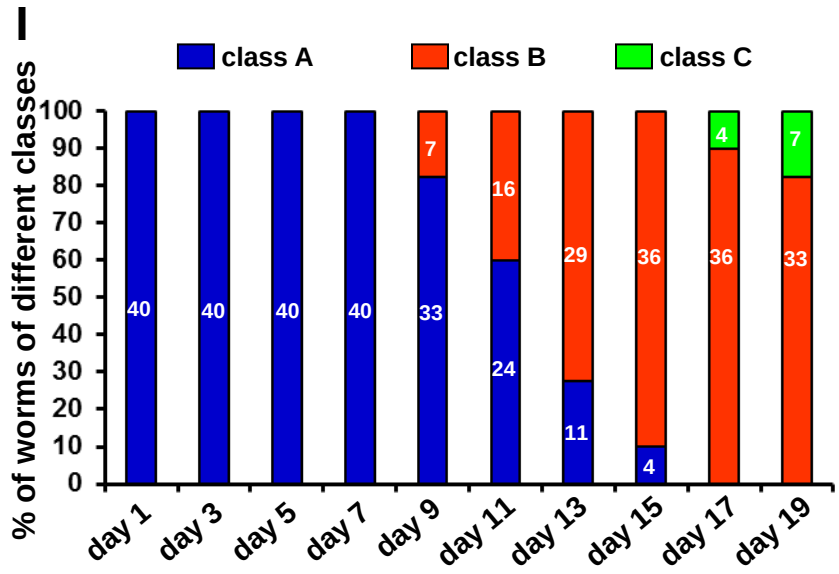

Figure S1, related to Figures 1. Locomotion speed and lifespan of WT and *daf-2* mutants. (A-B) WT worms. This is a replicate experiment of Figure 1. 20 worms were tracked each day for locomotion. Mean lifespan: 20.2±0.3 days (n=208/269); **(C-D)** *daf-2* mutants. 20 worms were randomly picked each day for locomotion analysis. Mean lifespan for *daf-2(e1368)*: 47.9±1.2 days (n=127/166); *daf-2(e1370)*: 52.2±1.4 days (n=121/173). **(E-F)** *daf-2* mutants. This is a replicate experiment of Figure S1C-D. Mean lifespan for *daf-2(e1368)*: 44.8±0.9 days (n=194/259); *daf-2(e1370)*: 50.3±1.2 days (n=167/272). **(G-H)** This analysis is a replicate of Figure 3J but using the data in Figure S1B and S1F. The rate of progressive decay in locomotion speed is greatly reduced in aging *daf-2(e1370)* and *daf-2(e1368)* worms. **(I)** Percent of WT worms in class A, B, and C analyzed for locomotion. As worms age, the population of class A decreases while that of class B and C increases. See the definition of class A, B and C worms in (Herndon *et al*., 2002). The N numbers of worms in each class are embedded in the bars. This data is a summary of Figure 1B and S1B. A similar result was obtained for *daf-2* (not shown). All error bars: SEM

Figure S2

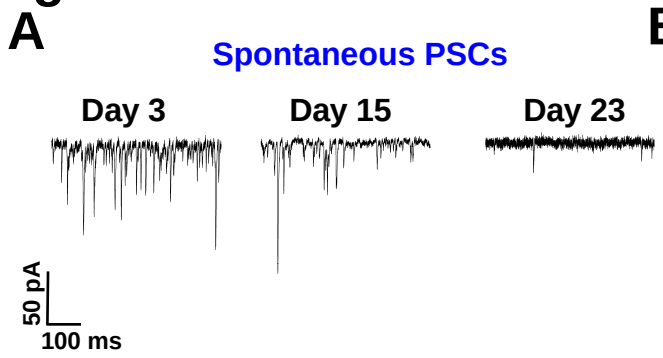

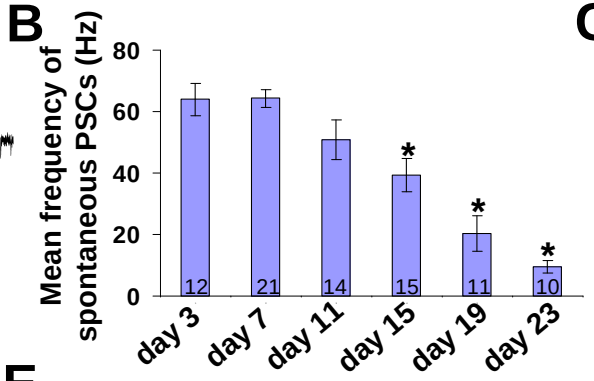

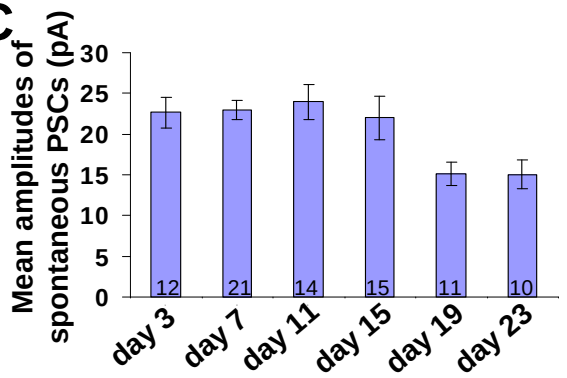

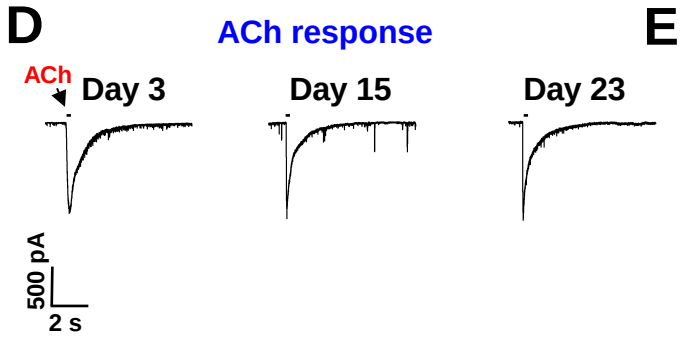

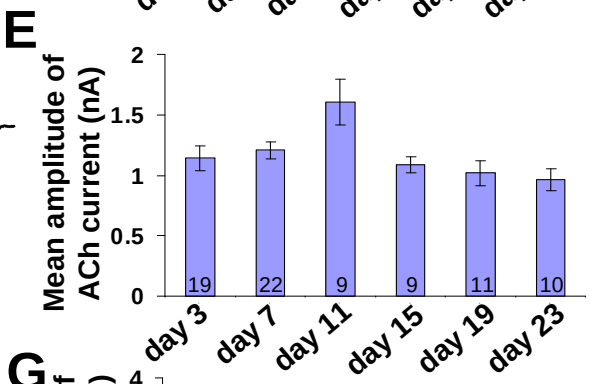

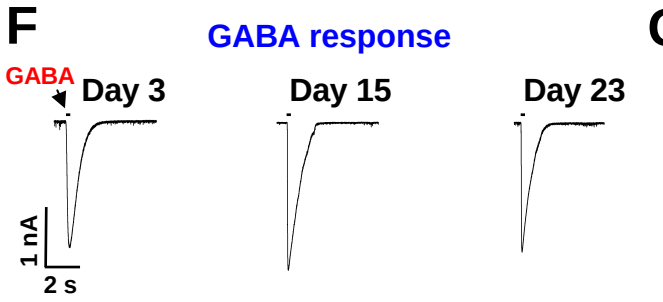

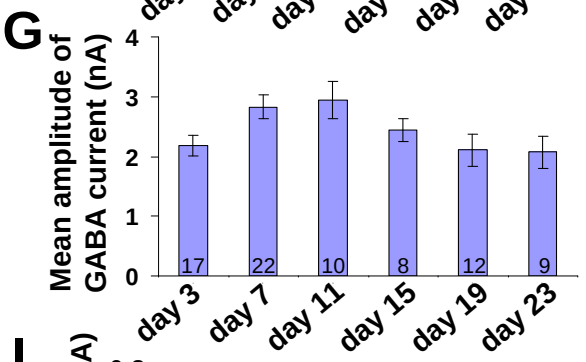

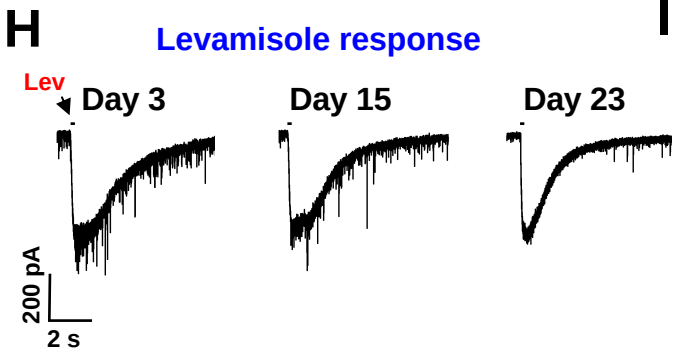

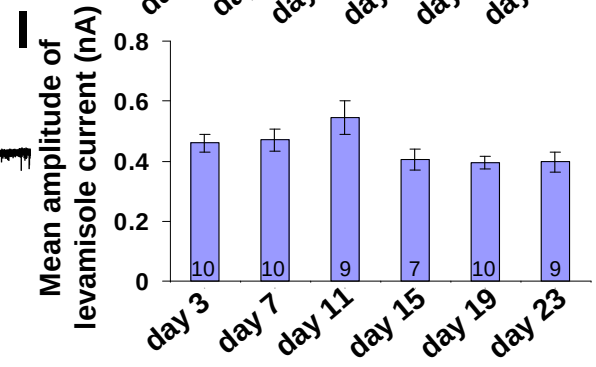

Figure S2, related to Figure 3. Patch-clamp recording of NMJs in aging *daf-2(e1368)* worms.

(A) Sample traces of endogenous PSCs recorded from the ventral cord NMJ of aging *daf-2(e1368)* worms. **(B)** Frequency of spontaneous PSCs recorded from aging *daf-2(e1368)* worms throughout lifespan. *p<0.0005 (ANOVA with Dunnett test). Error bars represent SEM. **(C)** Amplitude of spontaneous PSCs recorded from aging worms throughout lifespan. **(D)** Sample traces of body-wall currents evoked by ACh. **(E)** Bar graph of ACh-evoked currents in body-wall muscle cells of aging worms. **(F)** Sample traces of body-wall currents evoked by GABA. **(G)** Bar graph of GABA-evoked currents in body-wall muscle cells of aging worms. **(H)** Sample traces of body-wall currents evoked by levamisole. **(I)** Bar graph of levamisole-evoked currents in body-wall muscle cells of aging worms. Sample sizes (n numbers) are embedded in the bars of each graph. All error bars: SEM

Figure S3

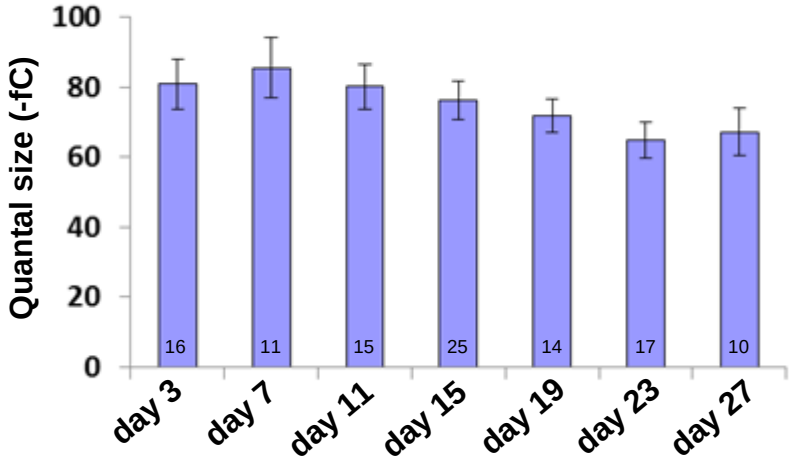

Figure S3, related to Figure 6. The quantal size of synaptic release measured in *daf-2(e1370)* animals. Sample sizes (n numbers) are embedded in the bars of the graph. All error bars: SEM.

Figure S4

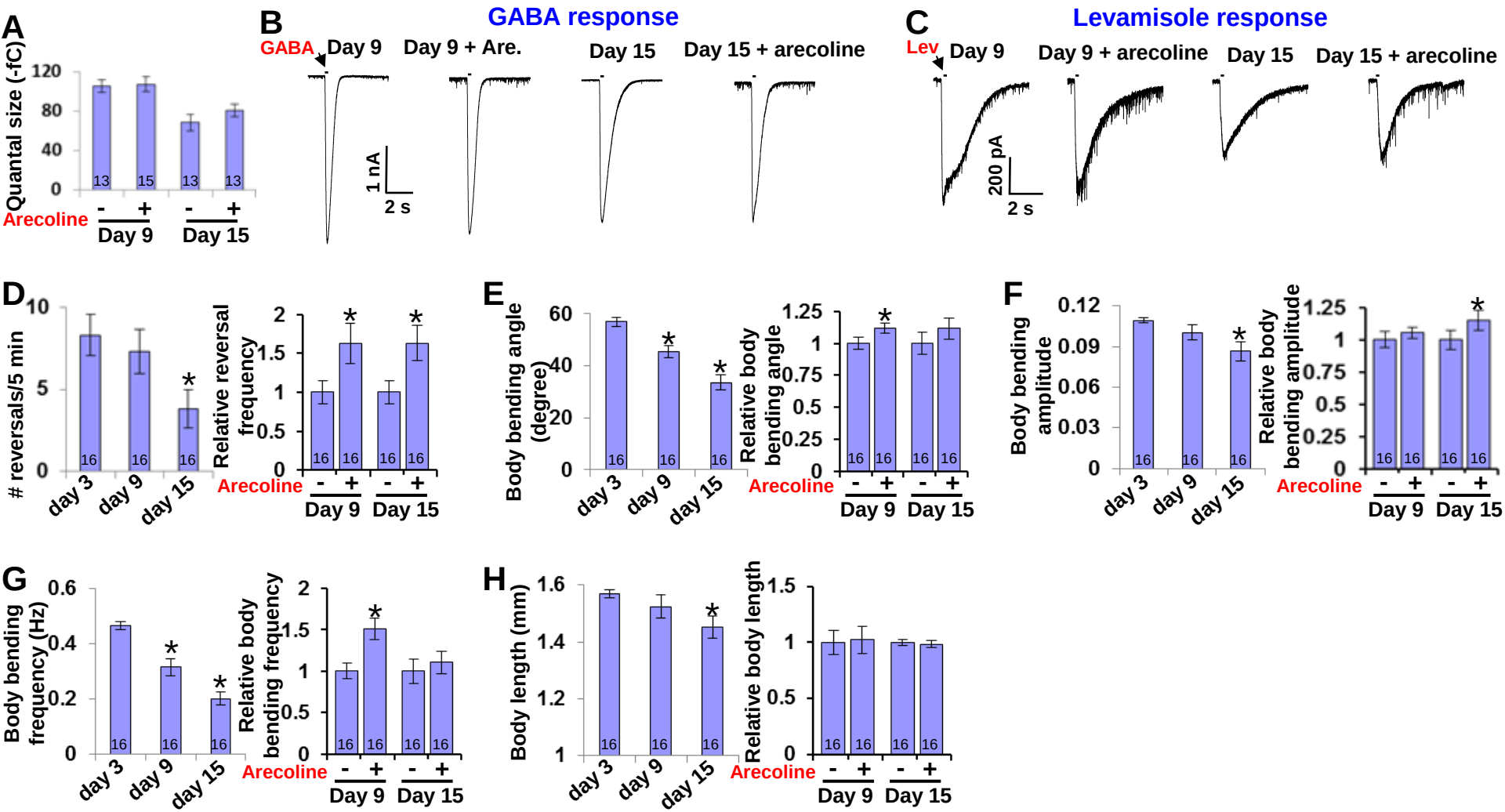

Figure S4, related to Figure 7. Additional data on the effects of arecoline on electrophysiology and locomotion parameters.
(A-C) Arecoline treatment does not alter the quantal size of synaptic release from motor neurons (A), GABA-evoked muscle currents (B), or levamisole-evoked muscle currents (C).

(D-H) The effects of arecoline on other locomotion parameters. We analyzed a number of additional locomotion parameters in aging worms, including reversal frequency (D), body bending angle (E), body bending amplitude (F), and bodying bending frequency (G). Day 9 and 15 worms show a decline in all these parameters compared to day 3 worms. Arecoline treatment can improve these parameters to varying degrees. As a control, we quantified a morphology parameter: the body length of the worm. Worms become shorter as they age. Arecoline treatment has no notable effect on this morphological parameter. Sample sizes (n numbers) are embedded in the bars of each graph. *p<0.05. All error bars: SEM.

Movie legends

Movie S1, related to Figure 7. Locomotion behavior of a day 9 worm prior to arecoline treatment.

Movie S2, related to Figure 7. Locomotion behavior of the same day 9 worm after arecoline treatment.

Movie S3, related to Figure 7. Locomotion behavior of a day 15 worm prior to arecoline treatment.

Movie S4, related to Figure 7. Locomotion behavior of the same day 15 worm after arecoline treatment.